

Selective Carbon–Carbon Bond Activation of Oxirane by a Bisphosphine Pt(0) Complex—A Theoretical Study

Philipp N. Plessow,^{†,‡,§} Jorge J. Carbó,^{§,||} Ansgar Schäfer,[‡] and Peter Hofmann^{*,||}

[†]Catalysis Research Laboratory (CaRLa), Im Neuenheimer Feld 584, D-69120 Heidelberg, Germany

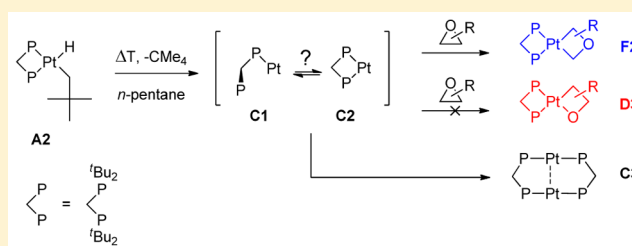
[‡]BASF SE, Quantum Chemistry, Carl-Bosch-Straße 38, D-67056 Ludwigshafen, Germany

[§]Department de Química Física i Inorgànica, Universitat Rovira i Virgili, 43007 Tarragona, Spain

^{||}Organisch-Chemisches Institut, Ruprecht-Karls-Universität Heidelberg, Im Neuenheimer Feld 270, D-69120 Heidelberg, Germany

S Supporting Information

ABSTRACT: Platinum(0) complexes with the chelate ligand bis(di-*tert*-butylphosphino)methane, ^tBu₂P-CH₂-P^tBu₂ (dtbpm), generated in solution from appropriate precursors, are the only known transition metal species that selectively activate epoxides (oxiranes) by inserting the Pt fragment into their carbon–carbon bond. The mechanism of this unprecedented reaction is studied theoretically using the random phase approximation. We find that the reaction is kinetically controlled and is caused by the formation of a monocoordinate (dtbpm- κ^1 Pt(0)) fragment rather than a (dtbpm- κ^2 Pt(0)) chelate complex. Insertion into epoxide C–C bonds occurs without energy barrier. Conceivable competing reactions, oxirane C–O and C–H activation, both proceed via formation of a σ -complex, followed by small but significant barriers for insertion steps. A reversible formation of the σ -complexes would perfectly explain the observed reactivity. For an irreversible formation, we find that intramolecular rearrangement of these σ -complexes toward C–C activation products is faster than both C–O and C–H activation. In principle, the same reactivity should be expected for other monocoordinated platinum(0) phosphine complexes. However, only the specific properties of dtbpm cause the subsequent, rapid, and irreversible closing of the chelate ligand yielding stable, square-planar Pt(II) C–C activation products.

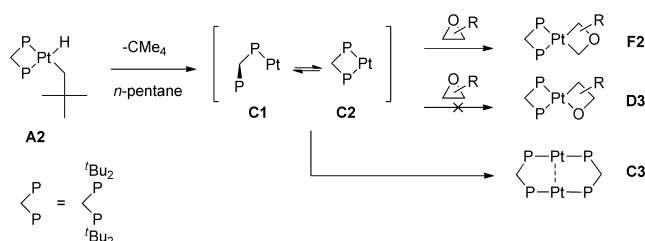


INTRODUCTION

Platinum complexes with the small bite-angle, bulky, and very electron-rich ligand bis(di-*tert*-butylphosphino)methane ^tBu₂P-CH₂-P^tBu₂ (dtbpm) show a unique reactivity toward epoxides: they selectively activate the C–C-bond. The stable neopentyl hydride complex (dtbpm- κ^2 Pt(Np)H) (A2) reductively eliminates neopentane already under ambient conditions and reacts with various epoxides to the corresponding 3-platinoxetanes F2 (see Scheme 1).^{1–3}

Kinetic measurements show¹ that the rate of these reactions corresponds precisely to that of a first-order elimination of neopentane from A2 both in absence and in the presence of epoxides and is practically independent of the solvent used

Scheme 1. Experimentally Observed Reactivity of (dtbpm- κ^2 Pt(Np)H) (A2)



($\Delta G^\ddagger \approx 100$ kJ/mol). This suggests a two-step process where neopentane is first eliminated in the rate-determining step and the generated [(dtbpm)Pt(0)] fragment (C1 or C2) reacts with epoxides in a very fast consecutive step.

Reactions with substituted epoxides of defined stereochemistry (*cis*- and *rac-trans*-2,3-dimethyloxirane) show that the reaction to the corresponding 3-platinoxetanes F2 occurs under retention of stereochemistry. This excludes free rotation around the C–O bonds on the reaction itinerary, which one would expect for a nonconcerted insertion of the metal fragment into the C–C bond via radical or zwitterionic processes. From experimental evidence, one would therefore deduce a concerted mechanism.¹

The elimination of neopentane from (dtbpm- κ^2 Pt(Np)H) (A2) in the absence of epoxides or other substrates occurs at approximately the same rate and results in dimerization of [(dtbpm)Pt(0)], giving a dtbpm-ligand bridged dinuclear structure (C3).^{4,5} Obviously, this reaction must occur under dissociation of one phosphorus ligand arm, and therefore the intermediacy of an open structure, [(dtbpm- κ^1 Pt(0))] (C1), has been hypothesized (and could not be excluded) from experimental data as a possibility. Due to the ring-strain of

Received: May 22, 2015

Published: July 26, 2015

dtbpm-complexes with a four-membered chelate bonding situation at the metal atom (angles P-M-P around 75°), such a reaction is more likely for this ligand than for other bisphosphine ligands with larger bite angles. While the basic properties of the closed chelate fragment, [(dtbpm- κ^2 P)Pt(0)] (C2), have already been described some time ago,⁶ C1 is expected to behave differently and its investigation as a reacting species by quantum chemistry at a state-of-the-art level has so far not been reported. Other activation reactions initiated by the elimination of neopentane from (dtbpm- κ^2 P)Pt(Np)H (A2) have been studied and C2 has been proposed as the reactive intermediate, but no direct experimental evidence for either intermediate C1 or C2 exists.^{4,5,7,8}

Carbon-carbon bond activation of epoxides has recently been studied for Rh(I) complexes but has been considered irrelevant in that context due to the thermodynamic instability of the product.⁹ Several metal-catalyzed reactions that are believed to proceed via 2-metallaoxetanes D3—(formally) C–O activated epoxides—have been reported and we refer to a recent review for details.¹⁰ The products of C–C activation, 3-platinoxetanes F2, have been prepared independently on other routes.^{11,12} Related reactions of strained alkanes, however, in particular of cyclopropanes, have been studied both experimentally and theoretically. The first activation of the cyclopropane carbon-carbon bond has been found already in 1955¹³ and many other examples including substituted cyclopropanes have been described since then.¹⁴ This reactivity pattern has been discussed in terms of the cyclopropane Walsh-orbitals¹⁵ and similar qualitative arguments can be made for oxirane due to the related orbital structure (see below). Notably, however, cyclopropane C–C bond activations with Pt as the metal work with Pt(II) complexes. Accordingly, C–C bond activation chemistry of cyclopropane is believed to require electrophilic transition metal complexes¹⁵ and reduction of the nucleophilicity of cyclopropane by substitution with electron-withdrawing groups has indeed led to a systematic decrease of the reaction rate.^{16,17} Interestingly, the reverse reactivity of the C–C activation of a cyclopropane, the elimination of 1,1-dimethylcyclopropane from a (Cy₃P)₂Pt-(3,3-dimethyl-cyclobutane) complex has been found to proceed via initial dissociation of a Cy₃P-ligand through a T-shaped d³-ML₃ species.¹⁸ In analogy, this could suggest C–C bond activation of epoxides via intermediate C1. In the context of epoxide C–C activation treated here, using the neopentyl hydride A2, we note parenthetically that this precursor also leads to direct insertion reactions of the [(dtbpm)Pt(0)] fragment (C1 or C2) into the C–C bonds of a wide variety of cyclopropanes. We will report this fascinating chemistry of C–C activations with Pt(0) separately.

It has been debated to which extent “activation strain” is responsible for relative barrier heights of C–C and C–H activation processes.¹⁹ However, it is self-evident that carbon-carbon bond activation is favored thermodynamically for strained reactants such as cyclopropane or epoxides. Furthermore, one should expect reduced barrier heights due to less “activation strain”, as the reactant is already strained. The insertion of metal complexes or metal atoms into cyclopropane C–C bonds has been studied by different authors. Early studies on palladium have been carried out by Siegbahn and co-workers.^{20–22} C–C bond activation barriers with atomic Palladium were found for cyclopropane to be lower than for ethane and also for cyclobutane by more than 63 kJ/mol. The insertion of the model complex (PH₃)₂Pd into the C–C bond

of a substituted cyclopropane has more recently been computed with a feasible barrier of 75 kJ/mol.²³

In this work we will study the reaction of (dtbpm- κ^2 P)Pt(Np)H (A2) with unsubstituted ethylene oxide (oxirane) to clarify the origin of the unusual reactivity. As we will show in this manuscript, the reactions studied are very fast and the activation barriers of competitive reactions differ by only very small amounts of energy. The same applies to the comparison of relevant energy minima. We will discuss the methods we use to compute sufficiently accurate energies first and continue with an investigation of the thermodynamics of the reaction in question. The equilibrium of proposed reactive intermediates, [(dtbpm- κ^1 P)Pt(0)] and [(dtbpm- κ^2 P)Pt(0)], (C1 and C2) will be discussed along with relevant molecular orbitals followed by investigation of the formation of these intermediates by reductive elimination of neopentane from the precursor, (dtbpm- κ^2 P)Pt(Np)H (A2). Finally, we will study how the fragments can react in various ways with oxirane and take a short look at related systems.

Computational Details. Molecular structures and thermodynamic gas-phase corrections, $\Delta G_{\text{gas,BP86}}$, were obtained at the BP86/def2-SV(P) level of density functional theory (DFT) using the resolution-of-the-identity (RI) approximation with appropriate auxiliary basis sets^{24–30} with TURBOMOLE.³¹ All calculations with Gaussian basis sets were carried out with effective core potentials³² for Pt to account for scalar relativistic effects.

The choice of method for geometry optimizations was not found to be too critical for the accuracy of the results: Reoptimization with B3LYP/def2-SV(P)³³ had no significant effect on reaction energies as compared to single point energies for the respective structures. The opposite is true for electronic reaction energies, where different methods give varying results for some reactions. Fortunately, model systems with smaller ligands, i.e., PH₃ or dhpm (*t*-butyl groups in dtbpm substituted by hydrogen atoms) can be studied for benchmark comparisons to gauge the accuracy of methods applicable to the real system. For systems of this size, coupled-cluster single point calculations at the CCSD(T)/def2-TZVPP level of theory are feasible, and D1-diagnostic (always <0.15, usually <0.10)³⁴ and basis set convergence compared to the def2-QZVPP³⁵ basis for CCSD indicate that this method is a good reference for benchmarking. Out of the conventional DFT-methods, typical hybrid functionals (B3LYP, M06⁴²) performed best in general, although, as also reported recently,³⁶ we found significant errors with M06 for oxidative additions. The best approach tested was to compute the correlation energy within the random phase approximation (RPA) based on PBE/def2-QZVPP KS orbitals^{37,38} using the implementation in the TURBOMOLE program package,^{39,40} and this is how absolute energies, E_{RPA} , were obtained throughout. In CCSD(T) and RPA calculations orbitals with orbital energies below $-3 E_h$ were frozen.

The influence of solvation was taken into account by computing free energies of solvation, $\Delta G_{\text{solv,M06}}$, with the SMD model⁴¹ and M06/def2-TZVP//BP86/def2-SV(P) single-point calculations with GAMESS-US^{42–45} for pentane as the least coordinating of the experimentally studied solvents. As one should expect, the influence of solvation was found to be in general rather small. The largest influence on reaction free energies (≤ 10 kJ/mol) was found when comparing free [(dtbpm)Pt(0)] fragments with their activation products of either oxirane or neopentane. The most important questions addressed in this manuscript involve mainly a comparison of

different activation routes, in general isomeric compounds. The impact of solvation on these reaction free energies was usually below 5 kJ/mol.

To summarize, we will discuss standard Gibbs free energies ($T = 298.15$ K; $c = 1$ mol/L) in pentane, G_{pentane} , computed as

$$G_{\text{pentane}} = E_{\text{RPA}} + \Delta G_{\text{gas,BP86}} + \Delta G_{\text{solv,M06}}$$

KS wave function analysis was carried out with ADF 2012.01⁴⁶ with single-point calculations at the BP86/TZ2P level of theory, treating relativistic effects with ZORA^{47–49} and the “small” frozen core option (Pt: 1–4s, 2–4p, and 3–4d; main group elements: all inner shells). The complexes were partitioned into epoxide and [(dtbpm)Pt(0)] fragments. All complexes and fragments were computed with closed-shell singlet KS wave functions. The relaxation of the fragment KS wave functions toward the interacting wave functions was studied in terms of gross occupation numbers on the basis of the fragment orbitals and by applying the bond-energy decomposition analysis^{50–54} as implemented in ADF.

RESULTS AND DISCUSSION

Thermodynamic Considerations of Overall Reactions.

Experimentally, reductive elimination of neopentane from the neopentyl-hydride complex **A2** gives either the dtbpm-bridged [(dtbpm)Pt(0)]₂-dimer **C3**, or—in the presence of epoxides—the C–C-activated products **F2**. According to our calculations, formation of the (dtbpm)Pt-dimer **C3** is exergonic with $\Delta G = -232$ kJ/mol⁵⁵ (i.e., -116 kJ/mol per monomer) relative to the precursor **A2**. C–O-activation of the epoxide is comparably favorable ($\Delta G = -115$ kJ/mol), C–C-activation is less favorable ($\Delta G = -54$ kJ/mol), and C–H-activation is least favored ($\Delta G = -28$ kJ/mol). We therefore conclude that the observed reactivity of epoxides has to be kinetically controlled.

Equilibrium and Structure of [(dtbpm- κ^1 P)Pt(0)] (C1) and [(dtbpm- κ^2 P)Pt(0)] (C2). Our calculations predict that **C1** rearranges with a barrier of only 44 kJ/mol to **C2**, which is less stable by 19 kJ/mol. These findings are similar to those for dhpm where they are supported by coupled-cluster calculations. The dangling phosphine arm upon dissociation from Pt is rotated out of the plane, which the four-membered chelate ring spans in **C2** (see Figure 1). This is reflected in the torsional

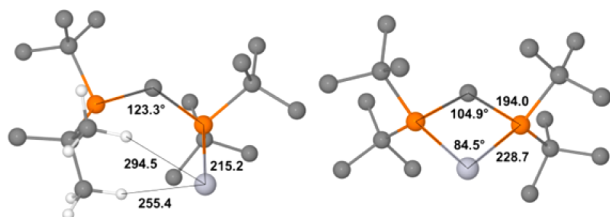


Figure 1. Computed structures of **C1** (left) and **C2** (right). Bond distances in pm, both are minimum energy structures.

angle defined by the ring atoms (Pt–P1–C–P2) which—upon dissociation of P2 from Pt—increases from 0.0° (**C2**) to 72.0° (**C1**). The small barrier (~ 20 kJ/mol) required for recoordination of the dangling phosphine arm is associated with the rotation around this torsional angle due to steric hindrance. This geometry and the barrier for recoordination are also observed for almost all three-coordinate, T-shaped Pt(II) complexes discussed below. The bite angle in the strained chelate **C2** is 84.5° about 10° larger than in many experimental structures of Pt(II)-dtbpm-complexes, such as **A2**. In the open

structure, the angle of the dtbpm backbone, $\angle(\text{P1}–\text{C}–\text{P2})$, increases from 104.9° (**C2**) to 123.3° (**C1**) and the P–Pt bond is shortened from 228.7 pm (**C2**) to 215.2 pm (**C1**).

Coordinationally unsaturated metal complexes are often stabilized by agostic interactions. A Bader analysis (BP86/TZ2P//BP86/def2-SV(P)) indeed shows bond paths to the two closest hydrogens for **C1**. On the other hand, the shortest Pt–H distance in **C1** is 255.4 pm, which is much longer than, for example, in the T-shaped (dtbpm- κ^1 P)Pt(Np)H-complex **A1** (215.4 pm, see below), where the agostic interaction is obvious. Furthermore, **A1** shows a significant elongation of the C–H bond (~ 2 pm) which is not the case for **C1**. It therefore seems unlikely that the stability of **C1** is caused by agostic interactions, as suggested in initial theoretical work.¹ This is in agreement with the fact that the properties of dhpm-complexes, which certainly do not have an agostic interaction, are similar. The short Pt–P bond (~ 220 pm) and the absence of agostic interactions (Pt–H distances ≥ 250 pm) are typical also for linear, two-coordinate Pt(0) complexes investigated below. An interesting feature of **C1** is that the dangling phosphine still shields the metal to some extent and can recoordinate rapidly and with low barrier, when a reaction takes place at the platinum(0) atom to give Pt(II) (see below).

Figure 2 shows the orbitals most relevant for the reaction. The HOMO–1 ($6a_1$) of the epoxide lies in the plane defined

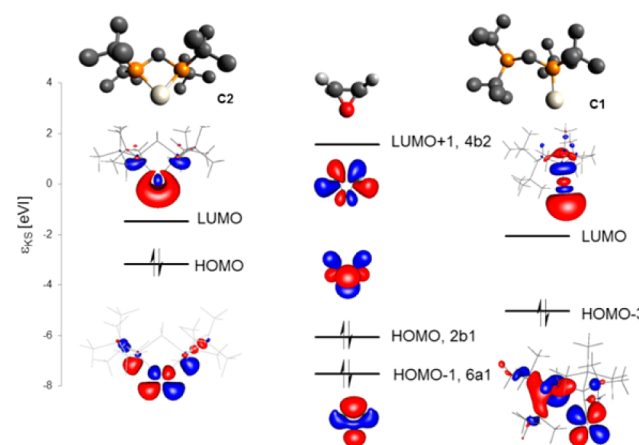


Figure 2. Relevant KS orbitals (BP86/def2-SV(P)) of [(dtbpm- κ^2 P)Pt(0)] (**C2**), oxirane, and [(dtbpm- κ^1 P)Pt(0)] (**C1**) with orbital energies, ϵ_{KS} , in eV. Hydrogen atoms of dtbpm have been omitted for clarity. For **C1** many occupied KS-orbitals have contributions from appropriate d-orbitals; only the one with highest energy is depicted.

by the C and O atoms and has the highest charge concentration at the C–C bond. The HOMO ($2b_1$) is essentially the out-of plane p-type oxygen lone pair (as beautifully visible in UV PE spectroscopy)⁵⁶ and is therefore expected to give rise to nucleophilic reactivity centered on the oxygen atom. Both $6a_1$ and $2b_1$ are suitable to donate charge via σ -type interactions into virtual orbitals (LUMO) of either **C1** or **C2**. This interaction is expected to be slightly stronger for **C1** which is more electrophilic, since the unoccupied orbital is clearly lower in energy (by 0.6 eV). The LUMO+1 ($4b_2$) of the epoxide has the right symmetry for accepting charge via in-plane π -interactions with the HOMO of **C2** or with two d-orbitals of **C1**. Here, **C2** is expected to be more reactive because the appropriate orbital for π -back-donation is higher in energy and **C2** is therefore more nucleophilic. Given the literature

precedent for electrophilic C–C bond activation of cyclopropanes,¹³ however, one should expect **C1** to be more reactive in C–C bond activation of epoxides as well.

Reductive Elimination of Neopentane from (dtbpm- κ^2 Pt(Np)H (A2). Although **C1** is—according to our calculations—certainly more stable, **C2** is accessible with a rather small barrier of 44 kJ/mol (see Figure 3). As the

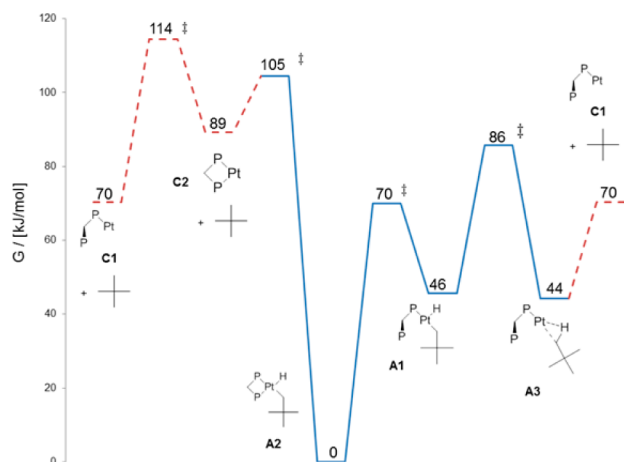


Figure 3. Free energy diagram (kJ/mol) for elimination of neopentane from A2 (center) and equilibration of [(dtbpm)Pt(0)] (**C1**, **C2**, left).

activation barriers for the reaction of the fragment with epoxides are of similar magnitude or even smaller (see below), it is important to find out if reductive elimination of neopentane from A2 gives **C1** or **C2**.

There are many cases known where metal complexes lose a monodentate ligand before reductive elimination reactions. For Pt(IV) complexes, even the opening of an unstrained chelate complex has been reported.⁵⁷ Reductive elimination without ligand dissociation is more common for Pt(II) complexes and has, for example, been found experimentally for (PPh₃)₂Pt(Me)H⁵⁸ and also in theoretical investigations of model complexes such as (PH₃)₂Pt(Me)H.^{59,60} For carbon–carbon bond formation by reductive elimination from Pd(II) complexes, a computational study has shown that, depending on the type of phosphine ligand, elimination from either three- or four-coordinated complexes can be favored.⁶¹ A general qualitative and elucidating analysis of reductive elimination from three- and four-coordinate d⁸-metal complexes at the extended Hückel level of theory was presented by R. Hoffmann and co-workers a long time ago.⁶²

According to our calculations, elimination after chelate ring opening via (dtbpm- κ^1 Pt(Np)H (**A1**) is more favorable ($\Delta G^\ddagger = 86$ kJ/mol) than via (dtbpm- κ^2 Pt(Np)H (**A2**) ($\Delta G^\ddagger = 105$ kJ/mol) and the barrier for κ^1/κ^2 isomerization of the neopentyl-hydride is certainly lower ($\Delta G^\ddagger = 70$ kJ/mol). This trend is observed for all computational methods tested. The underestimation of the barrier compared to the experimental barrier for reductive elimination is also found for a model system, (dhpm)Pt(Me)H, if one compares to coupled-cluster reference calculations. The errors for κ^1 (κ^2) are 6 (–3) kJ/mol. If one assumes a comparable error in the dtbpm system, it would give barriers of 92 kJ/mol (102 kJ/mol), which is in reasonable agreement with the experimental barrier of 100 ± 7 kJ/mol (in benzene).¹ Overall, all calculations indicate that elimination via a κ^1 -coordinated complex is more favorable and that formation of [(dtbpm- κ^1 Pt(0)] (**C1**) is therefore

favored kinetically and thermodynamically. Furthermore, relative to the precursor **A2**, the barrier for equilibration of **C1** and **C2** should already be slightly too high for this reaction to compete with the epoxide-activation reactions of **C1** (see below). As already noted above, **A1** exhibits an agostic interaction with a Pt–H distance of 215.4 pm (see Figure 4). This as well as the Pt–P bond distance of 238.4 pm are typical for the T-shaped (dtbpm- κ^1 Pt(II) complexes investigated here.

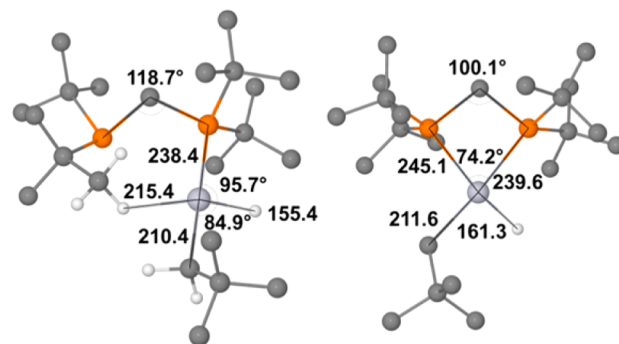


Figure 4. Computed structures of **A1** (left) and **A2** (right). Bond distances in pm.

We also tested whether an interaction with oxirane could facilitate the reductive elimination of neopentane. We obtained a four-coordinated complex [(dtbpm- κ^1 Pt(Np)H(C₂H₄O- κ^1 O)], which is endergonic by $\Delta G = 65$ kJ/mol relative to **A2**. The epoxide coordinates via the O-lone pair *trans* to the hydride. Our attempts to find a transition state (TS) for reductive elimination starting from this complex failed, since the oxirane always dissociated first, indicating that its coordination is not very strong in the first place.

Reaction with Oxirane. According to the considerations above, the κ^1 -fragment **C1** is formed first and is thermodynamically more stable. However, the κ^2 -fragment **C2** could be kinetically still be accessible and we have therefore studied the reactions of oxirane with both **C1** and **C2**. The epoxide can in principle be activated at the C–C, C–H, and C–O bonds, and we discuss all three possibilities below (for an overview, see Figure 5). Free energies will be given relative to the free oxirane and the more stable fragment, [(dtbpm- κ^1 Pt(0)] (**C1**), if not noted otherwise.

C–C Bond-Activation with [(dtbpm- κ^1 Pt(0)] (C1**).** Starting from separated molecules, the **C1** fragment can insert into the epoxide C–C-bond, without electronic energy barrier at the BP86/def2-SV(P) level of theory. This has been confirmed by single point energy calculations at the RPA PBE/def2-QZVPP level along the obtained path (see Figure 6). The same results are found for a [(PH₃)₂Pt(0)] + oxirane model system, where single point calculations at the coupled-cluster level were feasible. The platinum fragment attacks the epoxide C–C bond within the epoxide-molecular plane, along the P–Pt-bond axis. The epoxide-fragment is then asymmetrically bent to give the T-shaped activation product **F1** (see Figure 7). The dangling phosphorus arm recoordinates with a negligible barrier to give **F2** (see Figure 5), which makes the formation of **F1** essentially irreversible.

C–C Bond Activation with [(dtbpm- κ^2 Pt(0)] (C2**).** A path for insertion of this platinum fragment into the C–C bond can be obtained by a relaxed potential surface scan along

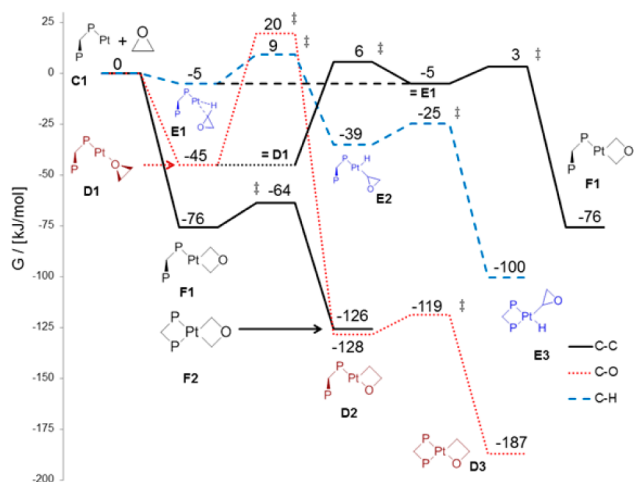


Figure 5. Free energy diagram (kJ/mol) for the reaction of (dtbpm- κ^1 P)Pt (C1) with oxirane.

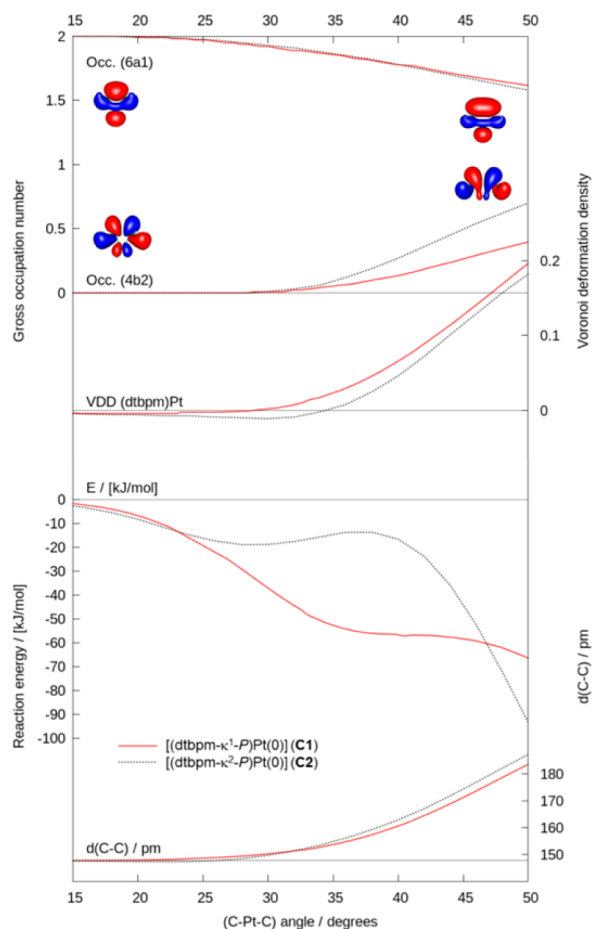


Figure 6. Observables and fragment analysis of the KS-wave function for the C–C activation of oxirane as a function of the $\angle(\text{C}–\text{Pt}–\text{C})$ angle for [(dtbpm- κ^2 P)Pt(0)] (C2, dotted blue line) and [(dtbpm- κ^1 P)Pt(0)] (C1, solid red line). From bottom to top: C–C distance of the epoxide fragment in pm, reaction energy in kJ/mol relative to the corresponding fragment (κ^1/κ^2), charge on the (dtbpm)Pt fragment according to Voronoi deformation density analysis and gross occupation numbers of the relevant epoxide fragment orbitals (4b₂, 6a₁).⁶³

different values of the $\angle(\text{C}–\text{Pt}–\text{C})$ angle, where C refers to the two epoxide carbons. The structures along the path exhibit C_2 -

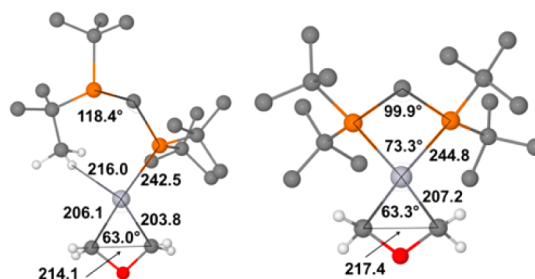


Figure 7. Computed structures of F1 (left) and F2 (right). Bond distances in pm.

symmetry. After a shallow minimum, a small barrier is passed. Relative to the [(dtbpm- κ^2 P)Pt(0)] fragment C2, only a slight activation barrier ($\Delta G^\ddagger = 20$ kJ/mol) is found, mainly due to entropic effects ($\Delta E^\ddagger = -14$ kJ/mol).

However, from the analysis above we know that C2 is unstable with respect to dissociation of one phosphorus arm. Extending the relaxed potential surface scan in one dimension above to a second dimension, which describes the $\kappa^2 \rightarrow \kappa^1$ process, shows indeed that the barrier for opening of the κ^2 -dtbpm ligand is very low in the vicinity of the TS (see Figure 8). The vibration corresponding to opening of a phosphine arm

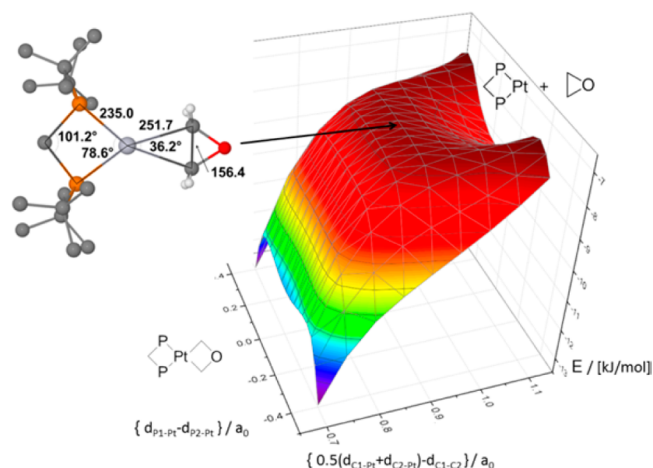


Figure 8. Reduced PES (BP86/def2-SV(P)) for the C–C activation of oxirane by [(dtbpm- κ^2 P)Pt(0)] (C2) as a function of the approximate reaction coordinate for C–C bond activation, $0.5(d_{\text{C1-Pt}} + d_{\text{C2-Pt}}) - d_{\text{C1-C2}}$, and of the coordinate for opening of a phosphine arm, $d_{\text{P1-Pt}} - d_{\text{P2-Pt}}$. Energy in kJ/mol, coordinates in a_0 .

is only 18 cm^{-1} at the TS. In fact, at the B3LYP/def2-SV(P) level of theory, the PES is slightly different, so that the TS and the C_2 -symmetric path in its vicinity are unstable with respect to symmetry-breaking. The curvature corresponding to opening of the phosphine arm becomes negative and the energy-maximum of the C_2 -symmetric path is a second-order saddle point. This indicates that interaction of the C–C bond with [(dtbpm- κ^2 P)Pt(0)] might as well result in an opening of the chelate, followed by C–C activation and recoordination of the dangling phosphine.

The energy-curves for C–C activation of the epoxide as a function of the C–Pt–C angle are compared for κ^1 and κ^2 fragments in Figure 6. Other structural properties, such as both Pt–C and the C–C bond distances, are very similar for both fragments along the path, so that the chosen angle is an appropriate coordinate to describe the reaction. As one can see

from Figure 6, the epoxide C–C distance is similar for the κ^1 and κ^2 fragments along the path and begins to exceed the equilibrium distance significantly around an $\angle(\text{C–Pt–C})$ angle of 30° . The energy profile is quite different: While there is a small but significant energy barrier for the κ^2 -fragment C2 at roughly 38° , the reaction energy for the κ^1 -fragment C1 is considerably negative with about -50 kJ/mol.

In order to understand these findings, the KS wave functions have been computed for the epoxide and the (dtbpm)Pt(0) fragments along the reaction path, and the relaxation toward the KS-determinant of the interacting molecule has then been studied. The orbital mixing is analyzed in terms of the gross occupation numbers of the occupied ($6a_1$) and unoccupied ($4b_2$) orbitals of the noninteracting epoxide fragment as basis functions in the interacting KS wave function (see Figure 6). At large separation, the epoxide and (dtbpm)Pt are of course not interacting, so that the occupation numbers equal those of the fragments, 2 and 0. Starting around $\angle(\text{C–Pt–C})$ of 20° , the occupation number of the $6a_1$ -orbital drops, indicating σ -interaction with the metal fragment. The occupation number of the virtual orbital suitable for π -back-donation toward the epoxide begins to rise at around an angle of 30° , precisely where the C–C bond length begins to increase. In an analysis of the charge flow that occurs upon relaxation of the noninteracting fragment densities, the Voronoi deformation density^{64,65} shows that, starting at around 30° , charge is significantly donated from the metal into the epoxide fragment, as one would expect for oxidative addition.

The different energy profiles of the C–C-activation of the two fragments for $\angle(\text{C–Pt–C})$ angles larger than 40° can be explained in terms of a more favorable π -orbital interaction/Pt–C bond formation that leads to a steeper energy curve toward the more stable product for the [(dtbpm- κ^2 Pt(0))] fragment C2. This is also reflected in a higher occupation of the $4b_2$ epoxide fragment orbital in the interacting KS wave function. The differing energy curve at $\angle(\text{C–Pt–C})$ angles smaller than 40° cannot—based on our data—be interpreted as arising from different σ -type interactions as the occupation of the $6a_1$ orbital (Figure 6) is basically identical. Further information can be gained by performing the bond energy decomposition analysis (EDA) as implemented in ADF, where the reaction energy can be broken up into several contributions (see Supporting Information for details). This analysis shows that the ‘orbital interaction energy’ is identical for C1 and C2 for $\angle(\text{C–Pt–C})$ angles smaller than 30° and becomes more favorable for C2 at larger angles. This is in agreement with our conclusion above, that σ -type interaction is similar and π -back-donation is more favorable for C2. According to the bond energy decomposition analysis, the difference in energy curves is due to Pauli repulsion and the energy required to bring the fragments from their equilibrium structure into the actual interacting geometry (“activation strain”), which is less favorable for C2.

C–O Bond Activation. According to our results, this conceivable process is preceded by the formation of the σ -complex D1, (dtbpm- κ^1 Pt)(C₂H₄O- κ^1 O), in which platinum is coordinated in a linear fashion by one dtbpm phosphorus atom and the epoxide oxygen atom (Figure 9). The bond formation can be understood as a Lewis acid/base reaction where the HOMO of the oxirane (essentially the out-of-plane oxygen lone-pair with some contribution from the CH₂-group orbitals, see Figure 2) interacts with the LUMO of the metal fragment of the right symmetry for interaction. There is an

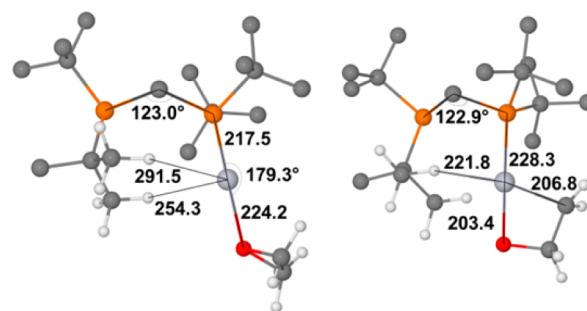


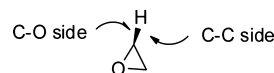
Figure 9. Computed structures of D1 (left) and D2 (right). Bond distances in pm.

additional interaction of the Pt-centered LUMO with the second oxirane sp^x -type lone pair located in the plane of the three-membered ring, not displayed in Figure 2. These two interactions explain the geometry of the complex, where the epoxide ring is significantly tilted with respect to the Pt–O axis. The complex D1 is formed without barrier if the epoxide attacks either C1 or C2, which means that we have not found a path for C–O activation without opening of the dtbpm chelate. We obtained a (dtbpm- κ^2 Pt)(C₂H₄O- κ^1 O) complex that is the transition state for exchange of the two phosphorus atoms, i.e., it connects the two isomeric, degenerate (dtbpm- $\kappa\kappa^1$ Pt)(C₂H₄O- κ^1 O) minima, D1.

Insertion of Pt into the C–O bond occurs roughly within the epoxide molecular plane and therefore requires a rotation of the coordinated epoxide. Relative to D1, the activation free energy barrier is 65 kJ/mol. Both possible isomers of the product, (dtbpm- κ^1 Pt)(C₂H₄O- κ^2 C₂O), are T-shaped, where the P-*trans*-C isomer is less stable ($G = -62$ kJ/mol) than the P-*trans*-O products, D2, ($G = -128$ kJ/mol), and the reaction barrier refers to the latter. The barrier required for subsequent recoordination of the dangling phosphorus of the dtbpm ligand is negligible.

C–H Bond Activation. The platinum atom can attack a C–H-bond from the side that is directed either toward or away from the epoxide oxygen (see Scheme 2).

Scheme 2. Possible Directions of Attack at an Oxirane C–H Bond



The first variant is slightly preferred ($\Delta\Delta G^\ddagger = 9$ kJ/mol) for the reaction with [(dtbpm- κ^1 Pt)(0)] (C1) and is the one depicted in Figure 5. The insertion into the C–H bond is preceded by the formation of a σ -complex E1 where the C–H bond is coordinated to platinum (see Figure 10). Formation of E1 is only slightly exergonic ($\Delta G = -5$ kJ/mol). The barrier for C–H activation relative to E1 is very low ($\Delta G^\ddagger = 14$ kJ/mol). The (dtbpm- κ^1 Pt)(C₂H₃O- κ^1 C)H complex formed, i.e., E2, readily reacts under coordination of the dangling phosphine arm to give E3.

C–H-activation starting from C2 is in general less favored but occurs also with a low barrier ($\Delta G^\ddagger = 18$ kJ/mol), relative to the [(dtbpm- κ^2 Pt)(0)] fragment C2. The activation barrier in this case is even lower than for the corresponding C–C activation. The barrier given for C2 refers to attack at the C–H

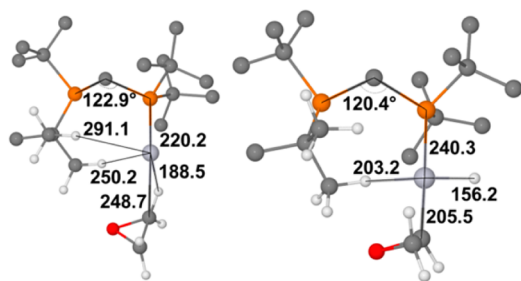


Figure 10. Computed structures of **E1** (left) and **E2** (right). Bond distances in pm.

bond on the side directed away from the oxygen, since attack on the other side led to dissociation of one phosphine arm.

Intramolecular Rearrangement of σ -Complexes for C–O and C–H Activation. The results above have shown that insertion into the C–C bond is irreversible and occurs without an energetic barrier. Formation of the σ -complexes **D1/E1** that must precede C–O/C–H activation also occurs without any barrier. Since we do not have access to possible free energy barriers,⁶⁶ none of these processes can be a priori excluded or considered as favored. The barriers for both C–O and C–H activation are only slightly above (<20 kJ/mol) the free energies of separate oxirane and [(dtbpm- κ^1 P)Pt(0)] fragments. Due to the principal error in the entropic contribution for condensation of molecules in solution, and since we cannot exclude a free energy barrier for dissociation/formation of the σ -complexes, it is not clear whether their formation is reversible or not.

If **D1/E1** are formed reversibly (as one would expect from a straightforward interpretation of Figure 5), the selectivity for C–C bond activation is easily explained in terms of the lower (nonexisting) barrier for insertion into the C–C bond. If **D1/E1** are formed irreversibly, this selectivity can at this point not be explained in simple terms since it is not clear why the formation of **D1/E1** should be disfavored.

We therefore studied intramolecular mechanisms for C–C activations starting from **D1/E1**. Our calculations (see Figure 5) show that the O-coordinated σ -complex **E1** with a lower barrier than that for C–O activation ($\Delta\Delta G^\ddagger = 14$ kJ/mol). **E1** rearranges to the C–C activated product **F1** with a barrier slightly lower than that for C–H activation ($\Delta\Delta G^\ddagger = 6$ kJ/mol).

In order to test the accuracy of the RPA for this particular problem, we computed the corresponding mechanism for Pt(PH₃) with single point calculations at the CCSD(T)/def2-QZVPP level of theory. The influence of the level of theory on the geometry was probed by reoptimizing the transition states with B3LYP/def2-SV(P) for dtbpm and B3LYP/def2-TZVPP for Pt(PH₃) and was again found to be negligible for relative barrier heights. For Pt(PH₃), C–O/(C–H) activation is disfavored by $\Delta\Delta G^\ddagger = 12(18)$ kJ/mol relative to C–C activation at the coupled-cluster level of theory. The RPA reproduces these results quite well: $\Delta\Delta G^\ddagger = 8(13)$ kJ/mol. Assuming the same systematic error for the dtbpm system increases the selectivity for C–C activation to $\Delta\Delta G^\ddagger \geq 11$ kJ/mol. We therefore believe in the significance of the energy differences, although they are certainly within the error range of conventional DFT methods.

In fact, a similar intramolecular rearrangement between Cp*(PMe₃)Rh(C₃H₅- κ^1 C)H and Cp*(PMe₃)Rh(C₃H₆- κ^2 C,C), the C–H and C–C activated complexes of cyclopropane, has

been found by Bergman et al.⁶⁷ Subsequent isotope labeling studies⁶⁸ have led to the hypothesis of an intermediate C–H σ -complex, similar to what we found above. However, while for the platinum complexes we find C–C activation to be thermodynamically and kinetically favored, C–H insertion is kinetically favored for the Rh complexes studied by Bergman, and rearrangement toward C–C activation takes place only at around 0 °C. We were therefore interested to see if our methodology can reproduce these results and we find indeed that the barrier for C–C activation is 18 kJ/mol higher than that for C–H activation in the Bergman system. The barrier for intramolecular rearrangement (88 kJ/mol) is in good agreement with the experiment.⁶⁹

Epoxide Activation in Related Systems. To see how the small bite-angle (84.5° in **C2**, 74.2° in **A2**) and chelate lability of the dtbpm-ligand affect the reactivity toward epoxides, we have studied 'Bu₂P–CH₂–CH₂–P'Bu₂ (dtbpe), the corresponding ligand with two methylene units in the backbone. The reactivity of the [(dtbpe- κ^2 P)Pt(0)] fragment is similar: It can activate C–C, C–H, and C–O bonds of epoxides with essentially the same ($\Delta G^\ddagger \approx 40$ kJ/mol) low barrier. The main difference is that the [(dtbpe- κ^1 P)Pt(0)] fragment is much less stable and probably of little importance. However, interestingly its computed chemistry is similar: It inserts into the epoxide C–C bond without an energy barrier, like Pt(PH₃) and [(dtbpm- κ^1 P)Pt(0)] **C1**. In this case, however, the chemistry should be determined by the closed chelate fragment [(dtbpe- κ^2 P)Pt(0)]. Although there is no experimental oxirane chemistry with dtbpe instead of dtbpm we are aware of, i.e., using a precursor analogous to **A2**, Whitesides et al. have studied the chemistry of the cyclohexyl system [(dcpe- κ^2 P)Pt(Np)H]^{70–72} and have found this precursor, after reductive elimination of neopentane, to exclusively C–H activate a wide variety of substrates. Unfortunately, epoxides were not looked at.

The homologous palladium(0) fragments [(dtbpm- κ^1 Pd(0))] or [(dtbpm- κ^2 Pd(0))] are also of interest, because when made from appropriate precursor compounds⁷³ they have been experimentally found to exclusively form the red d¹⁰–d¹⁰ Pd(0) dimer like **C3** mentioned in the beginning, without any activation of epoxides. The open structure (corresponding to **C1**) is computed to be 5 kJ/mol more stable than the closed structure (corresponding to **C2**). Our calculations show that the reactivity of [(dtbpm)Pd(0)] is similar to the Pt case, with the important difference that C–H and C–C activation products are much less stable and their formation is reversible. Even if they were formed, the activation products would therefore be expected to react to the more stable [(dtbpm)-Pd(0)]₂-dimer.

Our findings also resonate with the recent computational work on C–H bond activation by d¹⁰-M(L)_n complexes by Bickelhaupt et al.⁷⁴ The authors concluded that the behavior of Group 11 M(L)_n complexes is governed by a “ σ -regime”, in which the complex–substrate interaction is dominated by the orbital interaction of the occupied σ_{C-H} orbital and the unoccupied s-derived acceptor orbital of the metal complex.

CONCLUSIONS

We have shown that [(dtbpm- κ^1 Pt(0))] **C1** is thermodynamically more stable ($\Delta G = -19$ kJ/mol) than [(dtbpm- κ^2 Pt(0))] **C2** and is furthermore the kinetic product of the reductive elimination of neopentane from the precursor, (dtbpm- κ^2 Pt(Np)H) (**A2**). Reductive elimination occurs via

dissociation of one phosphorus atom trans to the hydride, followed by the actual reductive hydrocarbon elimination through σ -complex A3. This mechanistic picture concluded from theory—under the reasonable assumption, that the calculated numbers are reliable—solves a long-standing problem of $[(\text{dtbpm})\text{Pt}(0)]$ chemistry (and of some reactivity patterns of its Ni(0)- and Pd(0)-congeners) not amenable to an experimental solution. The original motivation and impetus to employ the dtbpm ligand was to create highly reactive $(\text{dtbpm}-\kappa^2\text{P})\text{M}(0)$ intermediates ($\text{M} = \text{Ni}, \text{Pd}, \text{Pt}$) with a four-membered chelate structure, as far as possible deviating from the linear groundstate geometry of $\text{d}^{10}\text{-ML}_2$ systems.

First, on the basis of qualitative MO theory considerations, $[(\text{dtbpm}-\kappa^2\text{P})\text{Pt}(0)]$ (C2) was believed to be the active species for various very unusual types of bond activation reactions when created from $(\text{dtbpm}-\kappa^2\text{P})\text{Pt}(\text{Np})\text{H}$ (A2) by elimination of neopentane or from other appropriate precursors. Soon, however, it became clear, that the reactivity of $[(\text{dtbpm})\text{Pt}(0)]$ (C) observed experimentally did not allow differentiation between $[(\text{dtbpm}-\kappa^2\text{P})\text{Pt}(0)]$ (14 VE, C2) and $[(\text{dtbpm}-\kappa^1\text{P})\text{Pt}(0)]$ (12 VE, C1). As mentioned in an accompanying experimental paper,¹ earlier attempts to tackle this question using theoretical methods did not allow any safe conclusions. We are confident that the level of quantum chemistry applied in the present work is sufficiently reliable to give a consistent interpretation of experimental findings. It is the $[(\text{dtbpm}-\kappa^1\text{P})\text{Pt}(0)]$ fragment C1, which inserts into the carbon–carbon bond of epoxides without a significant electronic energy barrier. Both C–O and C–H activation require an activation barrier and the first step in both cases is the formation of a σ -complex. A reversible formation of these σ -complexes would also selectively lead to C–C activation. The accuracy even of the methods applied here is insufficient to address this question of reversibility conclusively. However, we found that intramolecular rearrangement of the σ -complexes toward C–C activation is faster than both C–H and C–O activation. Therefore, irrespective of how epoxides and $[(\text{dtbpm}-\kappa^1\text{P})\text{Pt}(0)]$ (C1) react in a first step, successive C–C activation is favored.

The $[(\text{dtbpm}-\kappa^2\text{P})\text{Pt}(0)]$ fragment C2 would, according to our calculations, react with epoxides first under dissociation of one phosphorus arm of the four-membered chelate unit. Out of the reactions that retain bidentate coordination of dtbpm, C–H bond activation is slightly favored over C–C activation. Our results agree with the view in the literature that C–C bond activation of strained rings such as cyclopropanes is a reaction of electrophilic metal complexes. The electrophilic nature of the zerovalent $[(\text{dtbpm}-\kappa^1\text{P})\text{Pt}(0)]$ C1 is perhaps most evident in the formation of σ -complexes where the epoxide-oxygen or an epoxide C–H-bond coordinate to platinum.

Our calculations indicate that the preferred C–C bond activation of epoxides should also be expected for other monocoordinated Pt-phosphine complexes, such as $\text{Pt}(\text{PR}_3)$ or $[(\text{dtbpe}-\kappa^1\text{P})\text{Pt}(0)]$. However, the unique properties of dtbpm, which destabilizes small bite-angle Pt(0) chelate-complexes, make the formation of such a monocoordinate intermediate favorable. Also, fast stabilization of the C–C bond activated intermediates is required to avoid the reaction to thermodynamically more stable products. This is achieved by rapid recoordination of the dangling phosphine arm with its P center close to Pt. Finally, we note here, that the neopentyl hydride $(\text{dtbpm}-\kappa^2\text{P})\text{Pt}(\text{Np})\text{H}$ (A2) also easily C–C activates a large number of cyclopropanes to yield the corresponding

platinacyclobutanes. Here, a direct C–C activation without preceding C–H activation intermediates could be proven experimentally. The reactive species $[(\text{dtbpm}-\kappa^1\text{P})\text{Pt}(0)]$ C1 also explains the completely selective C–Si activation chemistry of organosilanes. These experimental findings and their theoretical background will be reported separately.^{75,76}

■ ASSOCIATED CONTENT

Supporting Information

Cartesian coordinates, absolute energies, gas-phase thermodynamic corrections, solvation free energies, and benchmark calculations. The Supporting Information is available free of charge on the ACS Publications website at DOI: 10.1021/acs.organomet.5b00435.

■ AUTHOR INFORMATION

Corresponding Author

*E-mail: ph@oci.uni-heidelberg.de.

Present Address

[#]Philipp N. Plessow, SUNCAT Center for Interface Science and Catalysis, Department of Chemical Engineering, Stanford University, Stanford, CA 94305, USA.

Notes

The authors declare no competing financial interest.

■ ACKNOWLEDGMENTS

P.N.P. worked at CaRLa of Heidelberg University, being cofinanced by Heidelberg University, the state of Baden-Württemberg and BASF SE. Support from these institutions is gratefully acknowledged. P.N.P. is grateful for having been invited to and hosted at Universitat Rovira i Virgili in Tarragona, where part of the work was carried out.

■ REFERENCES

- (1) Neumann, S.; Gerl, T. W.; Rominger, F.; Scherhag, G.; Meier, C.; Metz, M.; Hofmann, P. Selective Carbon–Carbon Bond Activation of Epoxides by a Bisphosphine Pt(0) Complex, *Organometallics* **2015**, submitted for publication.
- (2) Gerl, T. W. Dissertation; Technische Universität München: München, Germany, 1999.
- (3) Neumann, S. Dissertation; Ruprecht-Karls Universität Heidelberg: Heidelberg, Germany, 2000.
- (4) Hofmann, P.; Heiss, H.; Neiteler, P.; Müller, G.; Lachmann, J. *Angew. Chem., Int. Ed. Engl.* **1990**, *29*, 880–882.
- (5) Simhai, N.; Iverson, C. N.; Edelbach, B. L.; Jones, W. D. *Organometallics* **2001**, *20*, 2759–2766.
- (6) Hofmann, P.; Heiss, H.; Müller, G. *Z. Naturforsch., B: J. Chem. Sci.* **1987**, *42b*, 395–409.
- (7) Iverson, C. N.; Lachicotte, R. J.; Müller, C.; Jones, W. D. *Organometallics* **2002**, *21*, 5320–5333.
- (8) Hofmann, P.; Unfried, G. *Chem. Ber.* **1992**, *125*, 659–661.
- (9) Langer, N. N. P.; Bindra, G. S.; Budzelaar, P. H. M. *Dalton Trans.* **2014**, *43*, 11286–11294.
- (10) Dauth, A.; Love, J. A. *Chem. Rev.* **2011**, *111*, 2010–2047.
- (11) Hoover, J. F.; Stryker, J. M. *J. Am. Chem. Soc.* **1989**, *111*, 6466–6468.
- (12) Hoover, J. F.; Stryker, J. M. *Organometallics* **1989**, *8*, 2973–2975.
- (13) Tipper, C. F. H. *J. Chem. Soc.* **1955**, 2045–2046.
- (14) Campora, J.; Palma, P.; Carmona, E. *Coord. Chem. Rev.* **1999**, *193–195*, 207–281.
- (15) Crabtree, R. H. *Chem. Rev.* **1985**, *85*, 245–269.
- (16) McQuillin, F. J.; Powell, K. C. *J. Chem. Soc., Dalton Trans.* **1972**, 2123–2129.

- (17) Powell, K. G.; McQuillin, F. J. *Tetrahedron Lett.* **1971**, *12*, 3313–3316.
- (18) DiCosimo, R.; Whitesides, G. M. *J. Am. Chem. Soc.* **1982**, *104*, 3601–3607.
- (19) Diefenbach, A.; Bickelhaupt, F. M. *J. Phys. Chem. A* **2004**, *108*, 8460–8466.
- (20) Bäckvall, J. E.; Björkman, E. E.; Pettersson, L.; Siegbahn, P.; Strich, A. *J. Am. Chem. Soc.* **1985**, *107*, 7408–7412.
- (21) Blomberg, M. R. A.; Siegbahn, P. E. M.; Bäckvall, J. E. *J. Am. Chem. Soc.* **1987**, *109*, 4450–4456.
- (22) Siegbahn, P. E. M.; Blomberg, M. R. A. *J. Am. Chem. Soc.* **1992**, *114*, 10548–10556.
- (23) Suzuki, T.; Fujimoto, H. *Inorg. Chem.* **2000**, *39*, 1113–1119.
- (24) Weigend, F.; Ahlrichs, R. *Phys. Chem. Chem. Phys.* **2005**, *7*, 3297–3305.
- (25) Dirac, P. A. M. *Proc. R. Soc. London, Ser. A* **1929**, *123*, 714–733.
- (26) Becke, A. *Phys. Rev. A: At., Mol., Opt. Phys.* **1988**, *38*, 3098–3100.
- (27) Perdew, J. P.; Wang, Y. *Phys. Rev. B: Condens. Matter Mater. Phys.* **1992**, *45*, 13244–13249.
- (28) Vosko, S. H.; Wilk, L.; Nusair, M. *Can. J. Phys.* **1980**, *58*, 1200–1211.
- (29) Perdew, J. P. *Phys. Rev. B: Condens. Matter Mater. Phys.* **1986**, *33*, 8822–8824.
- (30) Armbruster, M. K.; Klopper, W.; Weigand, F. *Phys. Chem. Chem. Phys.* **2006**, *8*, 4862–4865.
- (31) TURBOMOLE v 6.4 2012, a development of University of Karlsruhe and Forschungszentrum Karlsruhe GmbH, 1989–2007, TURBOMOLE GmbH, since 2007; available from <http://www.turbomole.com> accessed 06/24/2015.
- (32) Andrae, D.; Haeussermann, U.; Dolg, M.; Stoll, H.; Preuss, H. *Theor. Chim. Acta* **1990**, *77*, 123–141.
- (33) Becke, A. D. *J. Chem. Phys.* **1993**, *98*, 5648–5652.
- (34) Jiang, W.; DeYonker, N. J.; Wilson, A. K. *J. Chem. Theory Comput.* **2012**, *8*, 460–468.
- (35) Weigend, F.; Furche, F.; Ahlrichs, R. *J. Chem. Phys.* **2003**, *119*, 12753–12762.
- (36) Lai, W.; Yao, J.; Shaik, S.; Chen, H. *J. Chem. Theory Comput.* **2012**, *8*, 2991–2996.
- (37) Perdew, J. P.; Burke, K.; Ernzerhof, M. *Phys. Rev. Lett.* **1996**, *77*, 3865–3868.
- (38) Perdew, J. P.; Burke, K.; Ernzerhof, M. *Phys. Rev. Lett.* **1997**, *78*, 1396–1396.
- (39) Eshuis, H.; Yarkony, J.; Furche, F. *J. Chem. Phys.* **2010**, *132*, 234114.
- (40) Eshuis, H.; Bates, J. E.; Furche, F. *Theor. Chem. Acc.* **2012**, *131*, 1084.
- (41) Marenich, A. V.; Cramer, C. J.; Truhlar, D. G. *J. Phys. Chem. B* **2009**, *113*, 6378–6396.
- (42) Zhao, Y.; Truhlar, D. G. *Theor. Chem. Acc.* **2008**, *120*, 215–241.
- (43) Schmidt, M. W.; Baldridge, K. K.; Boatz, J. A.; Elbert, S. T.; Gordon, M. S.; Jensen, J. H.; Koseki, S.; Matsunaga, N.; Nguyen, K. A.; Su, S.; Windus, T. L.; Dupuis, M.; Montgomery, J. A. *J. Comput. Chem.* **1993**, *14*, 1347–1363.
- (44) Feller, D. *J. Comput. Chem.* **1996**, *17*, 1571–1586.
- (45) Schuchardt, K. L.; Didier, B. T.; Elsethagen, T.; Sun, L.; Gurumoorthis, V.; Chase, J.; Li, J.; Windus, T. L. *J. Chem. Inf. Model.* **2007**, *47*, 1045–1052.
- (46) te Velde, G.; Bickelhaupt, F. M.; Baerends, E. J.; Fonseca Guerra, C.; Van Gisbergen, S. J. A.; Snijders, J. G.; Ziegler, T. *J. Comput. Chem.* **2001**, *22*, 931–967.
- (47) van Lenthe, E.; Baerends, E. J.; Snijders, J. G. *J. Chem. Phys.* **1993**, *99*, 4597–4610.
- (48) van Lenthe, E.; Baerends, E. J.; Snijders, J. G. *J. Chem. Phys.* **1994**, *101*, 9783–9792.
- (49) van Lenthe, E.; van Leeuwen, R.; Baerends, E. J.; Snijders, J. G. *Int. J. Quantum Chem.* **1996**, *57*, 281–293.
- (50) Ziegler, T.; Rauk, A. *Theor. Chim. Acta* **1977**, *46*, 1–10.
- (51) Ziegler, T.; Rauk, A. *Inorg. Chem.* **1979**, *18*, 1558–1565.
- (52) Ziegler, T.; Rauk, A. *Inorg. Chem.* **1979**, *18*, 1755–1759.
- (53) Morokuma, K. *J. Chem. Phys.* **1971**, *55*, 1236–1244.
- (54) Bickelhaupt, F. M.; Baerends, E. J. In *Reviews in Computational Chemistry*; Lipkowitz, K. B., Boyd, D. B., Eds.; Wiley-VCH: New York, 2000; Vol. 15, Chapter 1.
- (55) Due to the increased size of the molecule, this reaction free energy has been computed with RPA based on PBE/def2-TZVPP orbitals. Comparison with the other reaction energies (C–C, C–O and C–H bond formation) showed that the error is small for this purpose (5 kJ/mol).
- (56) Kimamura, K.; Katsumata, S.; Achiba, Y.; Yamazaki, T.; Iwata, S. *Handbook of He I Photoelectron Spectra of Fundamental Organic Molecules*; Japan Scientific Societies Press: Tokyo, 1981.
- (57) Crumpton-Bregel, D. M.; Goldberg, K. I. *J. Am. Chem. Soc.* **2003**, *125*, 9442–9456.
- (58) Abis, L.; Sen, A.; Halpern, J. *J. Am. Chem. Soc.* **1978**, *100*, 2915–2916.
- (59) Bartlett, K. L.; Goldberg, K. I.; Borden, W. T. *J. Am. Chem. Soc.* **2000**, *122*, 1456–1465.
- (60) Bartlett, K. L.; Goldberg, K. I.; Borden, W. T. *Organometallics* **2001**, *20*, 2669–2678.
- (61) Ananikov, V. P.; Musaev, D. G.; Morokuma, K. *Eur. J. Inorg. Chem.* **2007**, *2007*, 5390–5399.
- (62) Tatsumi, K.; Hoffmann, R.; Yamamoto, A.; Stille, J. K. *Bull. Chem. Soc. Jpn.* **1981**, *54*, 1857–1867.
- (63) Due to problems with the internal coordinates the activation path for (dtbpm- κ^1 P) has been computed in Cartesian coordinates, where the Pt–O distances has been used as a fixed coordinate.
- (64) Fonseca Guerra, C.; Handgraaf, J.-W.; Baerends, E. J.; Bickelhaupt, F. M. *J. Comput. Chem.* **2004**, *25*, 189–210.
- (65) Bickelhaupt, F. M.; van Eikema Hommes, N. J. R.; Fonseca Guerra, C.; Baerends, E. *Organometallics* **1996**, *15*, 2923–2931.
- (66) (a) Approximate free energy barriers can be obtained by computing free energies along an approximate reaction coordinate within the usual rigid-rotator/harmonic oscillator approximation, treating the forming/dissociating molecule(s) as one (super)molecule and omitting the vibration along the reaction coordinate, where the gradient is finite; see parts (b) and (c). For dissociation of both **D1** and **F1** we find no barriers, but dissociation to a constant free energy about 20 kJ/mol above free epoxide and **C1**. This is simply due to the different treatment of translation/rotation for two separate molecules and a supermolecule. This indicates that the free energy barrier should be below 20 kJ/mol or might also be nonexistent.. (b) Rasmussen, T.; Jensen, J. F.; Østergaard, N.; Tanner, D.; Ziegler, T.; Norrby, P.-O. *Chem. - Eur. J.* **2002**, *8*, 177–184. (c) Drudis-Sole, G.; Maseras, F.; Lledos, A.; Vallribera, A.; Moreno-Manas, M. *Eur. J. Org. Chem.* **2008**, *2008*, 5614–5621.
- (67) Periana, R. A.; Bergman, R. G. *J. Am. Chem. Soc.* **1984**, *106*, 7272–7273.
- (68) Periana, R. A.; Bergman, R. G. *J. Am. Chem. Soc.* **1986**, *108*, 7332–7346.
- (69) Solvation effects (*n*-pentane) are negligible, and we assume that this also applies to benzene, which has been used in the actual experiments.
- (70) Hackett, M.; Ibers, J. A.; Jernakoff, P.; Whitesides, G. M. *J. Am. Chem. Soc.* **1986**, *108*, 8094–8095.
- (71) Hackett, M.; Whitesides, G. M. *J. Am. Chem. Soc.* **1988**, *110*, 1449–1462.
- (72) Hackett, M.; Ibers, J. A.; Whitesides, G. M. *J. Am. Chem. Soc.* **1988**, *110*, 1436–1448.
- (73) The Pd(0) intermediate [(dtbpm)Pd(0)] can be made via reductive elimination of alkanes from [(dtbpm)Pd(Alkyl)]₂ precursors at ambient temperature. This chemistry will be published separately.
- (74) Wolters, L. P.; van Zeist, W.-J.; Bickelhaupt, F. M. *Chem. - Eur. J.* **2014**, *20*, 11370–11381.
- (75) Gerl, T.; Unfried, G.; Neiteler, P.; Metz, M.; Notheis, U.; Niemeyer, H.-H.; Pieper, G.; Scherhag, G.; Hofmann, P. *manuscript in preparation* 2015.

(76) Carbo, J. J.; Metz, M.; Brode, S.; Hofmann, P. *manuscript in preparation* 2015.